Scientific Research Publishing

Open Journal of Fluid Dynamics, 2024, 14, 205-223
https://www.scirp.org/journal/ojfd
ISSN Online: 2165-3860
ISSN Print: 2165-3852

The Effects of Fluid Structure Interaction (FSI) on a Baffle Hole in Mobile Storage Tank

Che Martin Ayiehfor, Ndapeu Dieunedort

Research Unit of Mechanics and Physical Systems Modelling (UR2MSP), Department of Physics, University of Dschang, Dschang, Cameroon
Email: cayiehfor@gmail.com, ndapeu@gmail.com

How to cite this paper: Ayiehfor, C.M. and Dieunedort, N. (2024) The Effects of Fluid Structure Interaction (FSI) on a Baffle Hole in Mobile Storage Tank. *Open Journal of Fluid Dynamics*, **14**, 205-223.
https://doi.org/10.4236/ojfd.2024.144010

Received: September 9, 2024
Accepted: December 1, 2024
Published: December 4, 2024

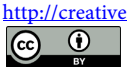

Abstract

Unsteady currents fluids flowing through a baffle with holes found in a mobile storage tank are complex to analyze. This study aims to evaluate the effects of fluid structure interactions (FSI) on baffles in tanks carried on mobile trucks that, more often than not, experience sloshing phenomenon engulfed by turbulences behaviors with respect to different motions of the truck. Mindful of the different types of baffles that are used in the tanks to limit sloshing wave activities and improve safety by allowing fluid to pass through carefully designed holes that are also placed in a specific pattern, the fluid structure interaction around a baffle with a hole is evaluated here through computing. Passing through the solver in COMSOL, an equivalent design tank and baffle with a hole is discretized to point form such that the fluid flowing through each point is evaluated and interpreted on a point graph generated with respect to each point located on the tank or baffle hole. The result obtained not only shows the effects of FSI as a function of turbulence kinetic energy per individual point but also the contour pressure field and velocity magnitude of the entire system.

Keywords

Fluid Structure Interaction (FSI), Baffle, Point Graph, Contour Pressure and Turbulence Kinetic Energy

1. Introduction and Notion of Fluid Structure Interactions (FSI)

The notion Fluid-Structure Interaction (FSI) is the multi-physics phenomenon of some movable or deformable structure with an internal or surrounding fluid flow in which the fluid flow interacts with a solid structure and exerts pressure and thermal loads onto the structure. Engineering sectors like the automobile, biomedical,

aeronautics, astrophysical, and environmental rely to a greater extent on FSI. FSI is a crucial consideration in the design of many engineering systems, e.g., automobiles, aircraft, spacecraft, engines, and bridges. Aircraft wings and turbine blades can break due to FSI oscillations. The startup of a rocket engine, like Space Shuttle Main Engine (SSME), experiences FSI, which sometimes leads to considerable unsteady side loads on the nozzle structure. A reed actually produces sound because the system of equations governing its dynamics has oscillatory solutions. The dynamic of reed valves used in two strokes engines and compressors is governed by FSI. The act of "blowing a raspberry" is another such example. The interaction between tribological machine components, such as bearings and gears, and lubricant is also an example of FSI. The lubricant flows between the contacting solid components and causes elastic deformation during this process. Fluid-structure interactions also play a major role in appropriate modeling of blood flow. Blood vessels act as compliant tubes that change size dynamically when there are changes to blood pressure and velocity of flow, and failure to take into account this property of blood vessels can lead to a significant overestimation of resulting Wall Shear Stress (WSS). In addition to pressure-driven effects, FSI can also have a large influence on surface temperatures in supersonic and hypersonic vehicles.

Fluid-structure interactions also occur in moving containers, where liquid oscillations due to the container motion impose substantial magnitudes of forces and moments on the container structure that affect the stability of the container transport system in a highly adverse manner. FSI can be stable or oscillatory. In oscillatory interactions, the strain induced in the solid structure causes it to move such that the source of strain is reduced, and the structure returns to its former state only for the process to repeat. In general, failing to consider the effects of FSI can be catastrophic, especially in structures comprising materials susceptible to fatigue, like those used in mobile storage tanks experiencing sloshing. Thus, the effects of sloshing forces in storage tanks being carried on trucks cannot be underestimated. In mobile storage tanks, Fluid motion can persist beyond application of a direct load to the container to a greater load similar to an exerted solid load of the same mass on the tank body.

Note that sloshing in tanks is felt more when they are partially filled. Sloshing exerts pressure on the walls of the tank, including the baffles such that if enormous, like in the case of an emergency braking or abrupt deceleration, they can create a heavier external thrust on the vehicle, which is considered to reduce the ability to maneuvering the vehicle by the driver at that critical moment was safety is needed. This is because the fluid moves to the front of the tank in the direction of forward movement due to momentum. This can be very catastrophic, particularly when the tank is occupied by petroleum volatile inflammable products. The effects of fluid sloshing forces in mobile tanks cannot be underestimated because, for every Fluid motion, there is turbulence and, consequently kinetic energy. This makes analysis linked to tank FSI and turbulent kinetic energy very important for mobile storage tanks.

Explicitly, the plashing of fluid on the walls of any given surface or part of the

tank is viewed as FSI, and since the fluid particles continually do not have a particular moving pattern to track them for evaluative studies, it becomes difficult to analyze. This makes analysis of sloshing in mobile tanks very important for mobile storage tanks.

The FSI model studies in this piece of work provide a coupled solution to the fluid dynamics in a baffle in mobile storage tanks as a stress evolution, fluid pressures, thermal gradients, and body forces contribute to deformations in the solid. Figure 1 below shows a picture of FSI on a magnified scale with a vivid elaboration of the fluid and the solid interface or boundary layer.

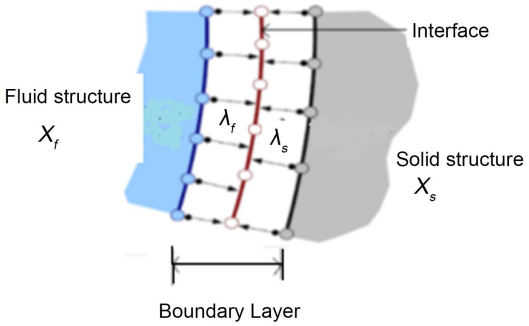

Figure 1. FSI interface.

Computerized study of FSI has proven to be efficient and faster in getting results in research nowadays with explicit vivid representation of fluid flow patterns for complex systems experiencing laminar or turbulence phenomenon. The following images in Figure 2 below represent samples of some computerized simulated models of FSI where 1) shows an example of laminar flow with a vertical obstruction in a channel, 2) shows a flow in a pipe with pressure or temperature variation being seen, 3) indicates the turbulence behavior of fluid flow in a system with a deformable barrier, 4) portrays fluid flow in a channel with a rotor and 5) highlight the variation of temperature and/or pressure on a fan blade.

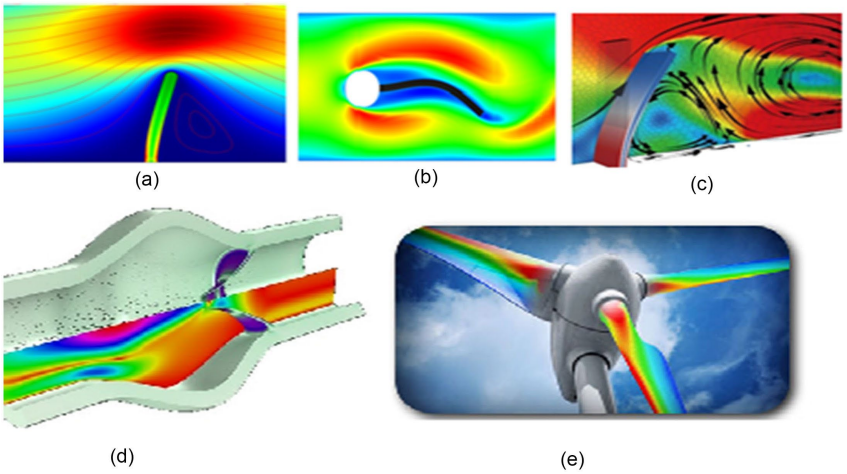

Figure 2. Examples of a computerized FSI. (Source: Comsol and Veryst engineering models)

Thus, the effects of FSI problems have become relevant when these scales are significant in influencing the physics of each domain interdependently, hence requiring a coupled framework to solve the governing equations pertaining to various domains. Problems involving fluid structure interactions can be solved through a monolithic or a partitioned approach and Lagrangian Eulerian method [1]-[3]. Governing equations for the fluid and structure domains are solved simultaneously in the monolithic approach within one system of equations.

In the partitioned approach, the fluid and solid domains are solved separately in their respective solvers, and the exchange of field variables across the domains takes place through an interface. Thus, the coupled problem can be solved by means of separate grids, dedicated solvers, and algorithms for each domain. This makes the partitioned approach more flexible than the monolithic approach. However, this comes at an added expense, as the interface conditions need to be carefully handled, especially in cases of large structural deformations. Particle and Meshless methods, in which the motion of each fluid particle is followed in a Lagrangian framework, have been developed to exploit the potentialities of the Lagrangian approach. Lagrangian finite element formulations without remeshing for incompressible fluid flow have been proposed but with an applicability range limited to only slightly distorted meshes.

In the Lagrangian formulation, the Navier-Stokes equations are written in material coordinates, which are continuously updated with iterative procedures. Moreover, a method to track interfaces is not necessary because the interfaces are defined by the current position of the material points. One of the main advantages of the Lagrangian approach is that the convective term in the momentum conservation equation disappears. However, if a fixed finite element mesh is used and the positions of element nodes are updated as a consequence of the fluid flow, very soon, the element distortion becomes excessive, and the finite element mesh needs to be regenerated.

Baffles are partitions placed in mobile storage tanks to reduce the rate of surging or sloshing of the fluid and minimize the tendency to create unwanted thrust. They also help to make the tank structure rigid. According to resend findings conducted by C.M. Ayiehfor [4] as a continuation of this research on the effects of fluid sloshing on different baffle configurations in storage tanks transported on trucks during an emergency braking, March 2024.

See https://www.scirp.org/journal/paperinformation.aspx?paperid=131203.

The greatest dynamic sloshing surging occurs in mobile storage tanks when partially filled with liquid material, where sloshing waves initiated in storage tanks are a response to an action. The intensity of the response is usually directly proportional to the action, particularly if nothing is done in the pathway of the volume of fluid to reduce the reaction (baffled).

2. Literature Review

Many studies have been carried out in relation to baffles and FSI, with one of the

most recent based on different baffle designs usable in cylindrical and elliptical storage tanks carried by trucks often used for transporting inflammable liquid materials in Cameroon [4]. Here, investigations are carried out to evaluate their safest fluid sloshing damping response during emergency braking, where the magnitude of sloshing waves are the greatest. The uncontrolled fluid sloshing creates thrust on the walls of the tanks usually felt externally on the truck carrying the tank and capable of hindering driver's effort to maintain steer ability and improve safety during critical braking moments. The study first passes through COMSOL, to expose the safest margin of each baffle type at instantaneous fluid pressure wave propagation initiated at a single phase to reflect sloshing in the storage tank during an emergency braking by the truck carrying the tank. The results are seen in the domain of acoustic Iso-surface pressure response, but acoustic pressure and sound pressure response are also seen automatically. Secondly, through an experimental finding in which fluid is forced to pass through each baffle and the resistance to fluid flow is measured as it's the baffle's damping ability. Either the fluid is lost through the baffle and by determination of the surface load exerted on each baffle due to the reaction of the residual fluid acting on the surface of each baffle after some of it is lost, the individual sloshing damping abilities are exposed. By comparing the experimental outcome with the computational response obtained, an ideal baffle design is proposed for cylindrical and elliptical tanks and is considered to respond to abrupt braking more efficiently.

Another analysis that focuses on FSI problems was done [5], in which the structure undergoes large deformations, and the fluid motion is characterized by free surfaces and breaking waves, which is of great relevance in many areas of engineering. Generally, the equations of motion for a Newtonian fluid are presented in Eulerian form; this formulation allows for the convenient solving of many situations with a fixed domain or control volume. Otherwise, the Arbitrary Lagrangian Eulerian method (ALE), in which the movement of the fluid particles is separated from that of the mesh nodes, is often applied. Typical difficulties of free-surface flow or fluid-structure interaction problems using Eulerian or ALE formulations are the treatment of the convective terms, the modeling of the wave splashing and the tracking of the free-surfaces and of the interfaces between fluids and structures which require dedicated algorithms, such as the volume of fluid.

A study on Lagrangian finite element method for the analysis of incompressible Newtonian fluid flows was also carried out [5], based on a continuous re-triangulation of the domain in the spirit of the so-called Particle Finite Element Method in which they revisited and applied the analysis of the fluid phase in fluid-structure interaction problems. It was considered a new approach for tracking the interfaces between fluids and structures, as proposed. Special attention here is devoted to the mass conservation problem. It is shown that, despite its Lagrangian nature, the proposed combined finite element-particle method is well suited for large deformation fluid-structure interaction problems with evolving free surfaces and breaking waves. The method is validated against the available analytical and numerical benchmarks.

In a related issue, a method is presented for the solution of the incompressible fluid flow equations using a Lagrangian formulation. The interpolation functions are those used in the Meshless Finite Element Method (MFEM) and the time integration is introduced in a semi-implicit way by a fractional step method [6]. Classical stabilization terms used in the momentum equations are unnecessary due to the lack of convective terms in the Lagrangian formulation. Furthermore, the Lagrangian formulation simplifies the connections with fixed or moving solid structures, thus providing a very easy way to solve fluid-structure interaction problems.

Over the last twenty years, computer simulation of incompressible fluid flow has been based on the Eulerian formulation of the fluid mechanics equations. However, it is still difficult to analyze problems in which the shape of the interface changes continuously or in fluid-structure interactions with free-surfaces where complicated contact problems are involved. More recently, Particle Methods in which each fluid particle is followed in a Lagrangian manner have been used [1]-[3] & [5].

An approach paper "titled Fluid-Structure Interaction Using the Particle Finite Element Method, 15 March 2006" is used to solve FSI problems [6]. Here both, the equations of motion for fluids and for solids have been approximated using a material (lagrangian) formulation. To approximate the partial differential equations representing the fluid motion, the shape functions introduced by the Meshless Finite Element Method (MFEM) have been used. Thus, the continuum is discretized into particles that move under body forces (gravity) and surface forces (due to the interaction with neighboring particles). All the physical properties such as density, viscosity, conductivity, etc., as well as the variables that define the temporal state such as velocity and position and also other variables like temperature are assigned to the particles and are transported with the particle motion. The so called Particle Finite Element Method (PFEM) provides a very advantageous and efficient way of solving contact and free-surface problems, highly simplifying the treatment of fluid-structure interactions.

Irrespective of all these beautiful research findings mentioned here in relation to this subject matter, adequate information has been established on the effects of FSI on baffle found in tanks but not still enough. It is in this line of thought that through this paper a more deeper and vivid finding are elaborate to explain the phenomenon FSI on a baffle in a storage tank as a function of turbulence kinetic energy per individual point on the baffle, and also the contour pressure field and velocity magnitude of the entire system.

3. Theory of FSI and Baffles in Mobile Tanks

3.1. Equations of Motion for Fluid Dynamic Fluid Particle Positions Problem

The fluid particle position in a tank is studied by solving the Lagrangian form of the Navier-Stokes equations [1] [7]-[9]

Let X_i the initial position of a particle a time $t = t_o$ and let x_i the final position. Been $u_i\left(x_j, t\right) = u_i$ the velocity of the particle in the final position the

following approximate relation can be written:

$$x_i = X_i + f\left(u_i, t, Du_i/Dt\right). \tag{1}$$

Most often the material transported in mobile storage tanks having baffles transported on trucks is liquid. In this study, we supposed that these fluid are incompressible. Thus, conservation of momentum and mass for incompressible Newtonian fluids in the Lagrangian frame of reference are represented by the Navier-Stokes equations and the continuity equation in the final x_i position, as follows:

Mass conservation:

$$\frac{D\rho}{Dt} + \rho\frac{\partial u_i}{\partial x_i} = 0. \tag{2}$$

Momentum conservation:

$$\rho\frac{Du_i}{Dt} = -\frac{\partial}{\partial x_i}p + \frac{\partial}{\partial x_j}\tau_{ij} + \rho f_i, \tag{3}$$

where ρ is the density, p the pressure, τ_{ij} deviatoric stress tensor, f_i the source term (usually the gravity) and $\frac{D}{Dt}$ represents the total or material time derivative.

For Newtonian fluids the stress tensor τ_{ij} may be expressed as a function of the velocity field through the viscosity μ by

$$\tau_{ij} = \mu\left(\frac{\partial u_i}{\partial x_j} + \frac{\partial u_j}{\partial x_i} - \frac{2}{3}\frac{\partial u_l}{\partial x_l}\delta_{ij}\right). \tag{4}$$

For near incompressible flows $\frac{\partial u_i}{\partial x_j} \ll \frac{\partial u_k}{\partial x_l}$ the term:

$$\frac{2\mu}{3}\frac{\partial u_i}{\partial x_i} \approx 0, \tag{5}$$

and it may be neglected from Equation (4). Then:

$$\tau_{ij} \approx \mu\left(\frac{\partial u_i}{\partial x_j} + \frac{\partial u_j}{\partial x_i}\right). \tag{6}$$

In the same way, the term $\frac{\partial}{\partial x_j}\tau_{ij}$ in the momentum equations may be simplified for near incompressible flows as:

$$\begin{aligned}\frac{\partial}{\partial x_j}\tau_{ij} &= \frac{\partial}{\partial x_j}\left(\mu\left(\frac{\partial u_i}{\partial x_j} + \frac{\partial u_j}{\partial x_i}\right)\right) = \mu\frac{\partial}{\partial x_j}\left(\frac{\partial u_i}{\partial x_j}\right) + \mu\frac{\partial}{\partial x_j}\left(\frac{\partial u_j}{\partial x_i}\right)\\ &= \mu\frac{\partial}{\partial x_j}\left(\frac{\partial u_i}{\partial x_j}\right) + \mu\frac{\partial}{\partial x_i}\left(\frac{\partial u_j}{\partial x_j}\right) \approx \mu\frac{\partial}{\partial x_j}\left(\frac{\partial u_i}{\partial x_j}\right).\end{aligned} \tag{7}$$

Using Equation (7), the momentum equation can be finally written as:

$$\rho\frac{Du_i}{Dt} = \frac{\partial}{\partial x_i}p + \frac{\partial}{\partial x_j}\tau_{ij} + \rho f_i \approx -\frac{\partial}{\partial x_i}p + \mu\frac{\partial}{\partial x_j}\left(\frac{\partial u_i}{\partial x_j}\right) + \rho f_i \tag{8}$$

Note: Equation (3) or the equivalent for incompressible fluid flow Equation (8)

are non-linear. In eulerian formulations the non-linearity is explicitly present in the convective terms. In this Lagrangian formulation, the non-linearity is due to the fact that Equations (3) and (8) are written in the final positions of the particles, which are unknown.

Boundary conditions

On the boundaries, the standard boundary conditions for the Navier-Stokes equations are:

$$\tau_{ij} v_j - p v_i = \bar{\sigma}_{ni} \quad \text{on } \Gamma_\sigma$$

$$u_i v_i = \bar{u}_n \quad \text{on } \Gamma_n$$

$$u_i \zeta_i = \bar{u}_t \quad \text{on } \Gamma_t$$

where v_i and ζ_i are the components of the normal and tangent vectors to the boundary.

3.2. Surface Topographic Baffle Section in Tanks

Sloshing in tanks can lead to serious forces, heat and chemical reactions sometimes that are harmful and increasingly become dangerous if the tank is without baffles or having poor baffle configurations. The hypothetical implementation is that tank surfaces are not smooth and the material to tank contact are not without inhibitors or layers. In examining the surfaces of a material, it is possible to identify the different localized layers more or less deeper in to material. In **Figure 3** below, we see an enlarged view of a material surfaces of the baffle plate in a tank are similar to this. Thus there are four layer before you get to the parent material.

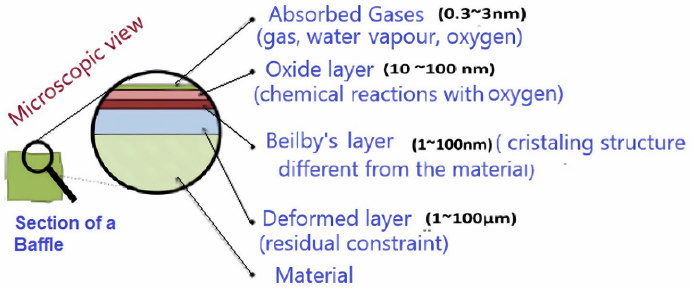

Figure 3. Microscopic view of Surface topography of a Baffle.

3.3. Tank Baffle Solid Dynamics Problems

The structure of the tank walls and baffle in particular will be considered as a rigid solid. Then, the equations of motion for a rigid body will be given by:

$$m \frac{DU_i}{Dt} = F_i \tag{9}$$

where F_i are the resultant of the external forces (surface forces, gravity force, etc.), whose line of action passes through the mass center of the body, U_i is the velocity of the mass center and m the total mass of the solid.

The actual motion of the rigid body consists in the superposition of the translation produced by the resultant force F_i and the rotation produced by the

couple T_i satisfying:

$$\frac{DM_i}{Dt} = T_i, \tag{10}$$

where M_i is the angular momentum about the mass center. It must be noted that in (10) the time derivative is expressed as the rate of change with respect to any non-rotating system of axis. It may be also expressed as the derivative with respect to the body fixed axes by:

$$\frac{DM_i}{Dt} \equiv \frac{\bar{D}M_i}{Dt} + \varepsilon_{ijk} e_i \Omega_j M_k = T_i, \tag{11}$$

where Ω denotes the angular velocity of the body, e are orthogonal unit basis vectors, ε the permutation symbol and $\bar{D}/Dt$ is the derivative with respect to the body fixed axes.

Let now the body fixed axes be the principal axes of inertia of the body, with its origin at the center of mass, then:

$$M_i = I_i \Omega_i, \text{ (without summation in the index } i) \tag{12}$$

where I_i are the principal moments of inertia and then:

$$\frac{\bar{D}M_i}{Dt} = I_i \frac{\bar{D}\Omega_i}{Dt}. \tag{13}$$

Finally, the equations of motion of the tank baffle body might be summarized as:

$$m\frac{DU_i}{Dt} = F_i, \tag{14}$$

$$I_i \frac{\bar{D}\Omega_i}{Dt} + \varepsilon_{ijk} e_i \Omega_j \left(I_k \Omega_k\right) = T_i, \tag{15}$$

Calling a_i and $\propto_i$ the linear and the angular acceleration of the mass center of the body:

$$m a_i = F_i, \tag{16}$$

$$I_i \propto_i + \varepsilon_{ijk} e_i \Omega_j \left(I_k \Omega_k\right) = T_i, \tag{17}$$

This is a non-linear system of partial differential equations that has to be linearized for its numerical approximation.

The final rigid body velocity of an arbitrary point is a combination of both, the linear velocity of the center of mass U_i and the angular velocity Ω_i according to:

$$u_i = U_i + \varepsilon_{ijk} e_i \Omega_j r_k. \tag{18}$$

where r_i is the distance from the origin of the body axes to an arbitrary point attached to the body. The velocity u_i will be used later as a boundary condition for the fluid dynamics problem.

A very large number of problems involve plane motion. In this case, equation (15) reduces to:

$$I\frac{\bar{D}\Omega}{Dt} \equiv I \propto = T, \tag{19}$$

where Ω, I, Ω and T are the planar angular velocity, the moment of inertia, the planar angular acceleration and the external couple respectively.

4. Method

With many references to other research works, the computerized study has proven to be explicit and closed to accurate. Reason why this study passes via COMSOL [10] being just one amongst many different types of software to simulate FSI problems Thus the investigation of effects of FSI on baffles in storage tanks seen here is based on the application of the principles of flow passed through a cylinder. Mindful of the fact that the flow of fluid behind a blunt body as experience in the tank baffle is difficult to compute due to the unsteady flows.

The wake behind such a body consists of unordered eddies of all sizes that create large drag on the body when you place a slender body at right angles to a slow the turbulence in the thin boundary layers next to the streamlined bodies strong disturbances of flow is notice. See [2] page 8 and [7].

4.1. Baffle in Tanks Development

Baffles seen in cylindrical or elliptical tanks mounted on trucks and used for transporting liquid material are often welded vertically in the tank and have holes that allow fluid flow to and fro (forth and pack) depending on the direction tank agitation due truck mobility phenomenon like rolling, yawing and pitching with significant intensities felt when the tank is partially filled. Both cylindrical and elliptical tanks have baffles as seen below in **Figure 4**.

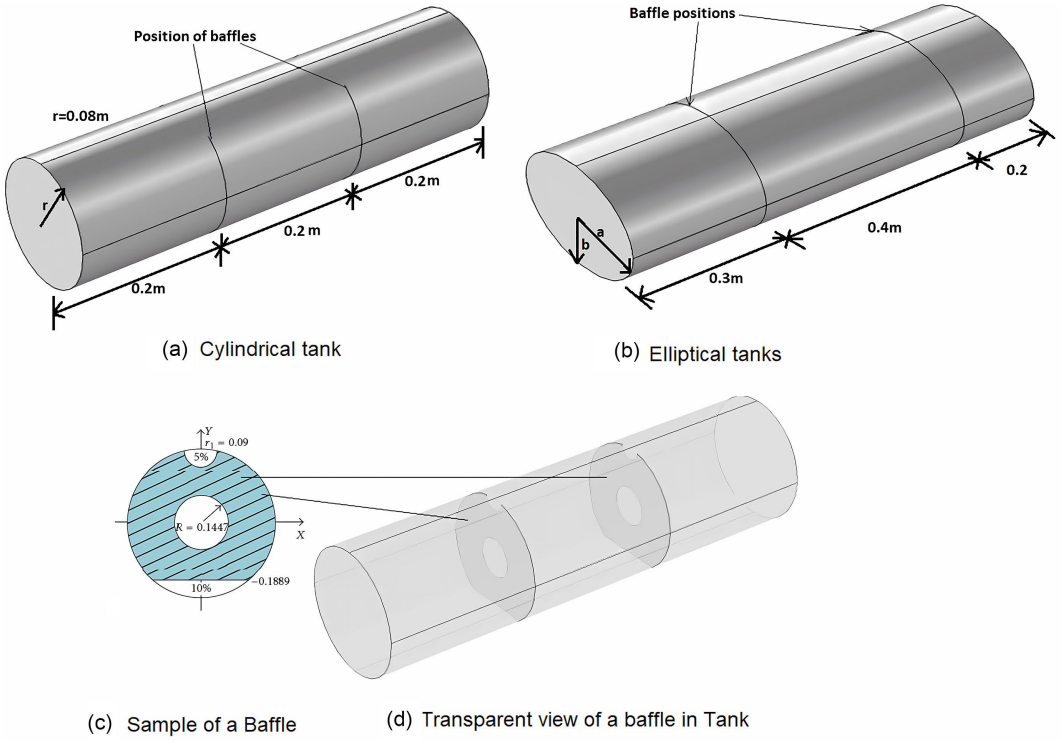

Figure 4. Description of tank and a baffle.

Many types of baffle designs are being used nowadays in mobile storage tanks. The application of any design depends on each manufacturer expected result but

must often than not, they consider the type of material to be carried in the tank, state of material to be maintained (liquid, solid or gas) during transportation, temperature and pressure factors.

The Figure 5 and Figure 6 below show the various baffles designs applicable for cylindrical storage and elliptical tanks respectively tanks with their sectional material surface extraction guide in percentage with respect to tank sizes to ease production.

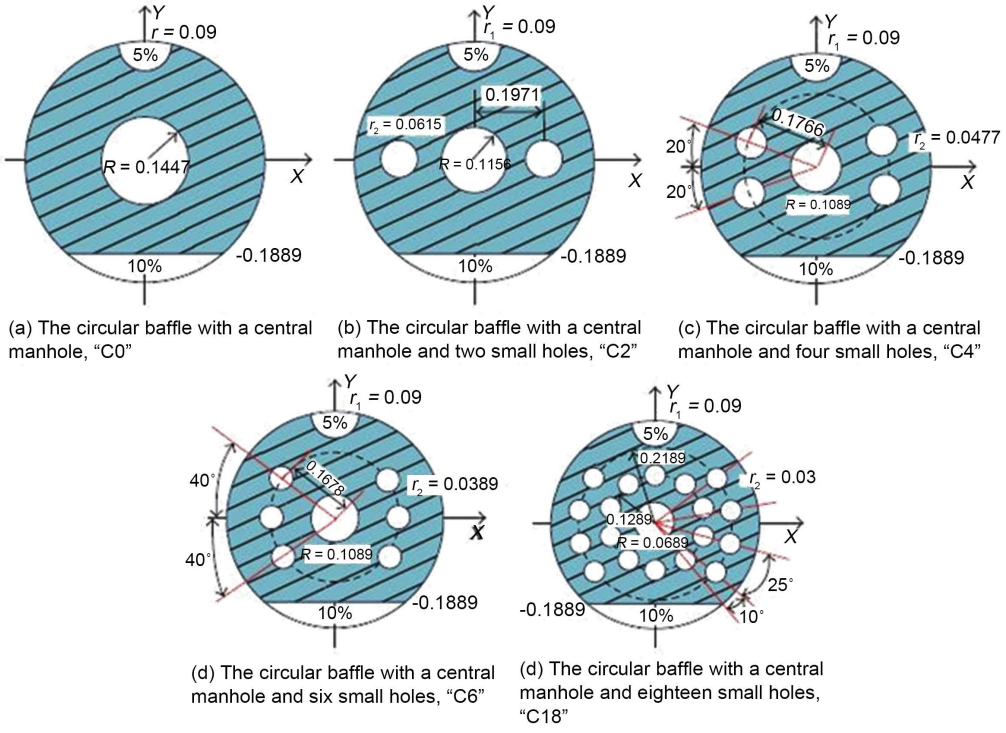

Figure 5. Various baffles designs for cylindrical tanks [4].

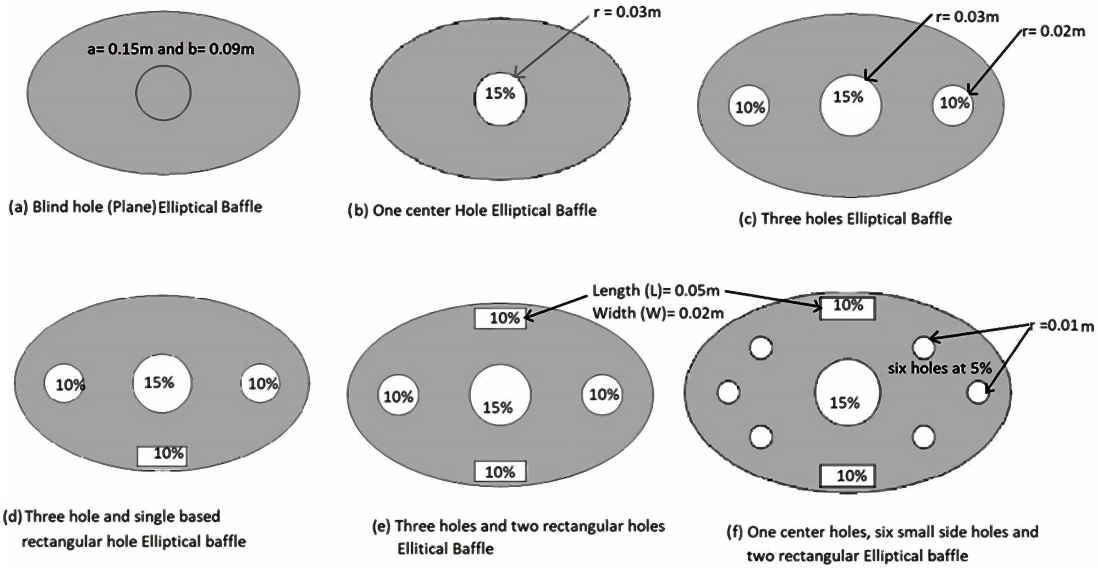

Figure 6. Various baffles designs for elliptical tanks [4].

4.2. Fluid Flow through a Baffle Hole

The model implemented here examines unsteady, incompressible flow past a long cylinder supposing to be placed in a channel at right angle to the oncoming sloshed fluid. With a symmetric inlet velocity profile, the flow needs some kind of asymmetry to trigger the vortex production. This can be achieved by placing the cylinder with a small offset from the center of the flow. In this case, an unstructured mesh is used, and the small asymmetry in the mesh proves to be enough to trigger the vortex production. A key predictor is the Reynolds number, which is based on cylinder diameter. For low values (below 100) the flow is steady. In this simulation, the Reynolds number equals 100, which gives a developed von Kármán vortex street, but the flow still is not fully turbulent.

The viscous forces on the cylinder are proportional to the gradient of the velocity field at the cylinder surface. Evaluating the velocity gradient on the boundary by directly differentiating the FEM solution is possible but not very accurate. The drag and lift forces themselves are not as interesting as the dimensionless drag and lift coefficients. These depend only on the Reynolds number and an object's shape, not its size. The coefficients are defined as using the following parameters:

$$C_D = \frac{2F_D}{\rho U_{mean}^2 L}$$

$$C_L = \frac{2F_L}{\rho U_{mean}^2 L}$$

where:

- F_D and F_L are the drag and lift forces
- ρ is the fluid's density
- U_{mean} is the mean velocity
- L is the characteristic length, in this case the cylinder's radius

The specific effect of fluid flow through a baffle hole is closely similar to the effects of fluid flow through a cylinder or pipe but with a very high diameter to length (thickness) ratio. But as a recall the outcome of fluid flow through a pipe is laminar, turbulent and or transitional as seen in Figure 7 below.

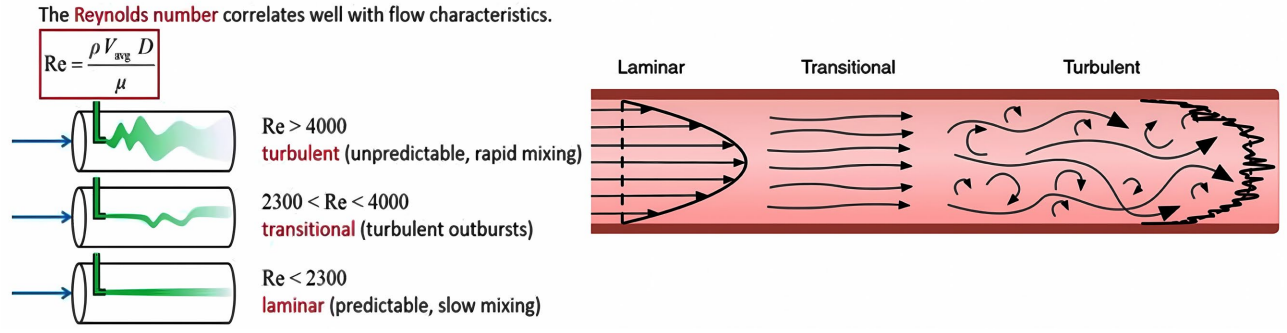

Figure 7. Laminar, transitional and turbulent patterns.

However, just after the baffle, the flow pattern can be very difficult to predict but depends on:

- Baffle hole surface finish.
- Cylindricity of the hole.
- Volatility of the fluid.
- Density of the fluid.
- Velocity of fluid flowing.
- After baffle material body distance obstructing resistance to flow such as air, same fluid in a different section or chamber with a different momentum another baffle.

Mindful of the fact that different designs of perforations of holes are applied on the baffle during manufacturing as indicated in earlier paragraphs, the hole could be in form of a square, rectangular, round or sectors and that some cases we have a combination of two or more types of the listed holes perforation on a single baffle. We now literally consider averagely that what ever the type perforations or hole design on either the cylindrical or elliptical tank baffles, when viewed from the side and in a two dimensional perspective, as applied in this study, the cross sectional view is as seen in Figure 8 below.

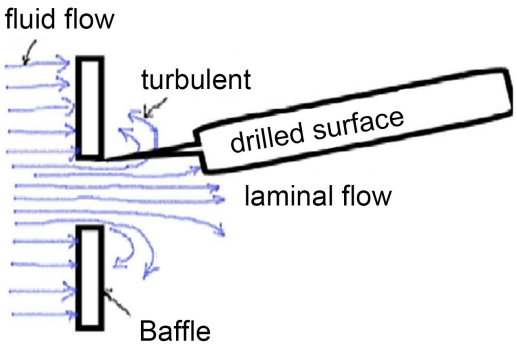

Figure 8. Fluid flow behavior through a baffle hole [4].

4.3. Turbulent Kinetic Energy Theory

In fluid dynamics, turbulence kinetic energy (TKE) is the mean kinetic energy per unit mass associated with eddies in turbulent flow. Physically, the turbulence kinetic energy is characterized by measured root-mean-square (RMS) velocity fluctuations. In the Reynolds-averaged Navier Stokes equations, the turbulence kinetic energy can be calculated based on the closure method otherwise called turbulence model [11]-[16]. In summary, TKE helps to:

- Turbulent kinetic energy measures the intensity of turbulence in a flow.
- Turbulent budget terms help in identifying the stability or irresoluteness of the flow.
- Dissipation occurs when the eddies interact and the viscous force converts kinetic energy into heat.

Analytically TKE can be defined as being half the sum of the variances σ^2

(square of standard deviations σ) of the fluctuating velocity components:

$$k = \frac{1}{2}\left(\sigma_u^2 + \sigma_v^2 + \sigma_w^2\right) = \frac{1}{2}\left[\overline{(u')^2} + \overline{(v')^2} + \overline{(w')^2}\right]$$

where each turbulent velocity component is the difference between the instantaneous and the average velocity: $u' = u - \overline{u}$ being Reynolds decomposition. The mean and variance are

$$\overline{u'} = \frac{1}{T}\int_0^T \left(u(t) - \overline{u}\right) \mathrm{d}t = 0,$$

$$\overline{(u')^2} = \frac{1}{T}\int_0^T \left(u(t) - \overline{u}\right) \mathrm{d}t \geq 0 = \sigma_u^2, \text{ respectively.}$$

During sloshing in the storage tank, the fluid passing through the baffle hole and TKE is produced by fluid shear, friction or buoyancy, or through external forcing at low-frequency eddy scales (integral scale). This turbulence kinetic energy is then transferred down the turbulence energy cascade, and is dissipated by viscous forces at the Kolmogorov scale. This process of production, transport and dissipation can be expressed as: $\frac{Dk}{Dt} + \nabla \cdot T' = \varepsilon$,

where:

- $\frac{Dk}{Dt}$ is the mean-flow material derivative of TKE
- $\nabla \cdot T'$ is the turbulence transport of TKE
- P is the production of TKE
- ε is the TKE dissipation.

Haven outline the above notions and with respect to this study were computational fluid dynamics (CFD) is applied, it is impossible to numerically simulate turbulence without discretizing the flow-field as far as the Kolmogorov microscales in which we have the smallest scales in turbulent flow were viscosity dominates and the turbulence kinetic energy is dissipated into thermal energy. This is the bases of the COMSOL solver of TKE.

4.4. Computing

The above explanations on fluid flow via a baffle equivalent to FSI and turbulent kinetic theory is a linkup to the understanding our findings and acts as a guide to designing, dimensioning and computing [17]-[19]. It should be recalled that our specific focus is on fluid structure effects applied on a baffle hole hence, the influence of baffle size to tank size is not consider in this findings and an arbitrary tank size has been applied. Thus the dimensions of the baffle under test are 0.05 m in thickness by 0.4 m in height as seen in the following image of **Figure 9**

From an engineering standpoint, it is important to predict the frequency of vibrations at various fluid speeds and thereby avoid undesirable resonances between the vibrations of the solid structures and the vortex shedding. Depending on the type, a baffle in a tank can have many designs of holes. For the purpose of this study, our focus is strictly on a single hole evaluated at macroscopic scale and computed.

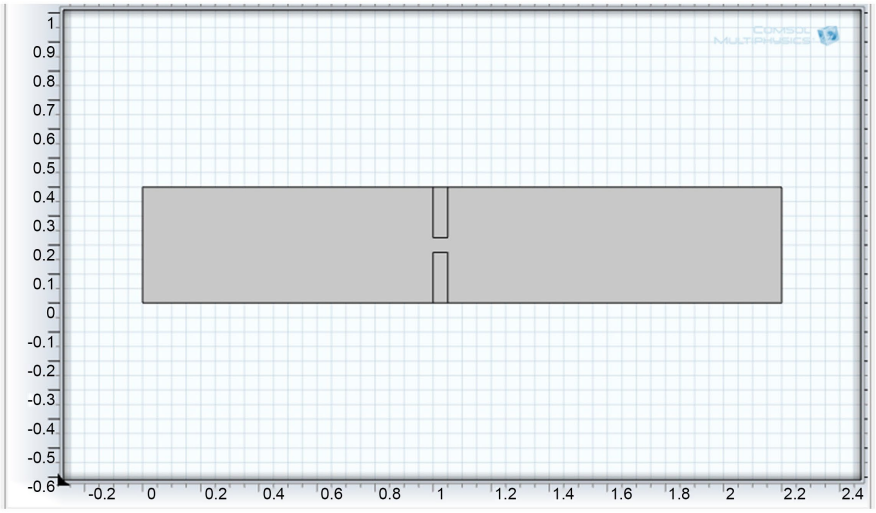

Figure 9. Basic 2D tank and baffle design under FSI study.

Identification of Points

In the model builder of COMSOL, a series of steps are taken to obtain these result. It begins with imputing global definitions, model, definition of parameters, geometry of the baffle, materials, turbulent flow variables, meshing and study. The outcomes are result in function of data set, velocity, pressure and plot group carrying the point graph. Here the various points are auto generated from the geometry such that during study, it analyses the behavioral characteristics of the fluid flow nature on that point and generate the graph termed the "point graph". The **Figures 10-12** below shows an example of point 5 and other points follow suit. Hence, to identify the other point developed entails just pinpointing the point with the cursor under the plot menu in the solver and if shall be highlighted.

5. Results

The model system was generated, build and computed within the tank safe working pressure (see page 31 of [4] for safe working pressure notes) the and following picture of **Figure 13** was realized for surface velocity magnitude developed in the tank with the baffle as the center and that of **Figure 14** was also obtained as a description of initiated contour pressure in the tank before the baffle.

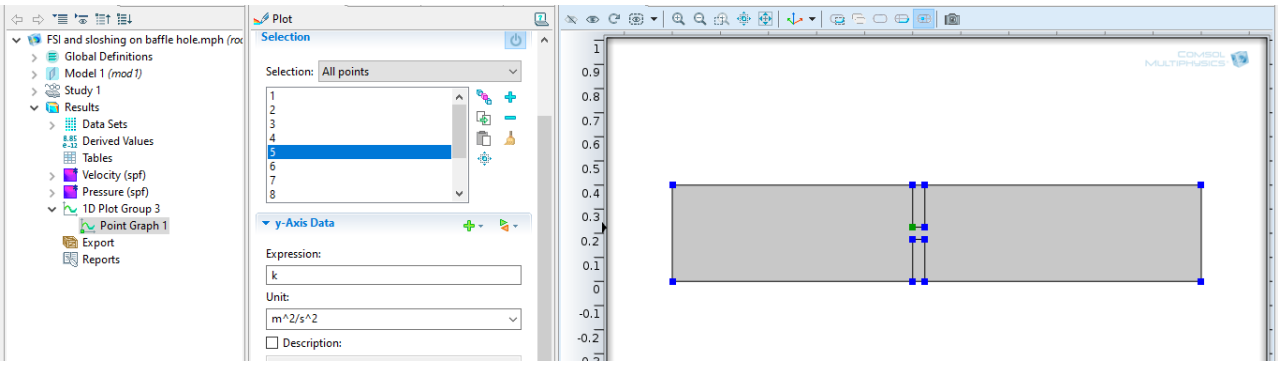

Figure 10. Identification of point.

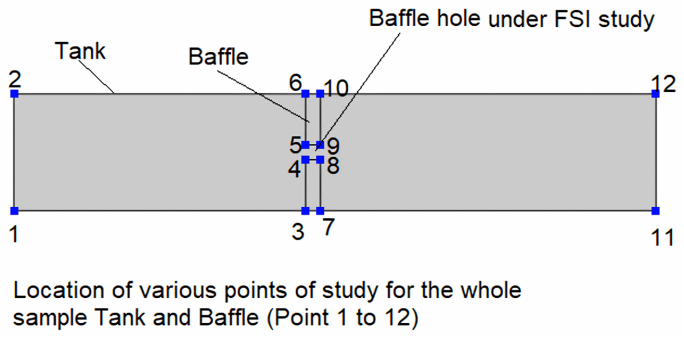

Figure 11. FSI study points for both tank and baffle during activated fluid flow.

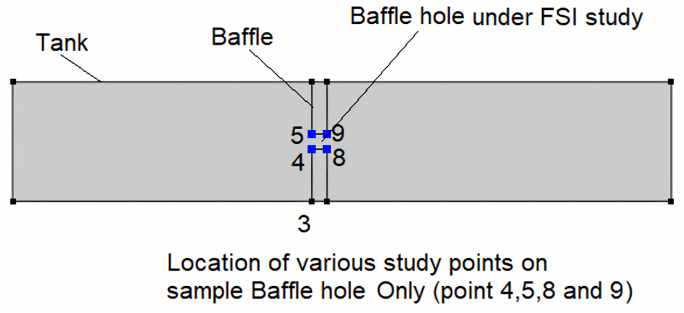

Figure 12. FSI study points for only the baffle hole during activated fluid flow.

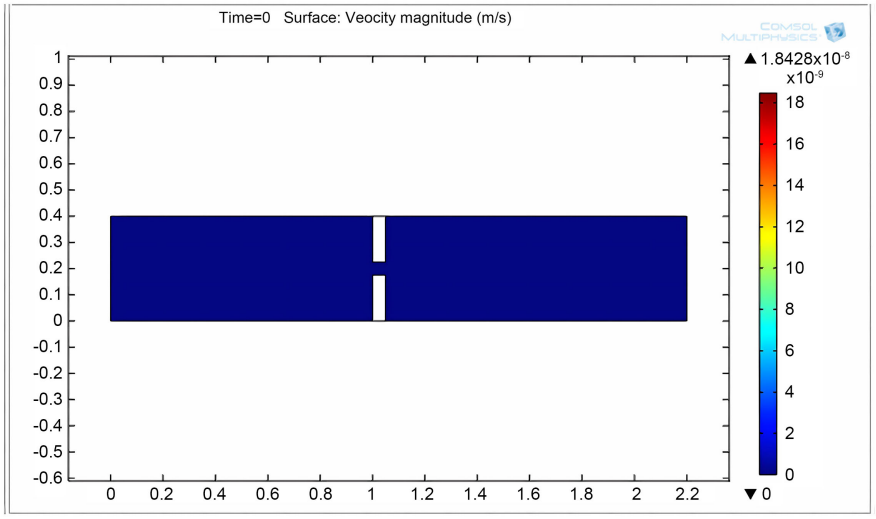

Figure 13. Velocity magnitude behind and in front the baffle in tank.

The following graphs are the out come of the the computed study with each representing the tubulent kinetic energy per point around the baffle hole with respect to the initiated pressure expressed with respect to time. Figure 15 represent an evaluation of the whole system of point from 1, 2,3, … to 12. While Figure 16 is a part evaluation with focus only on point 4, 5, 8 and 9 being the baffle hole experiencing fluid flow during sloshing.

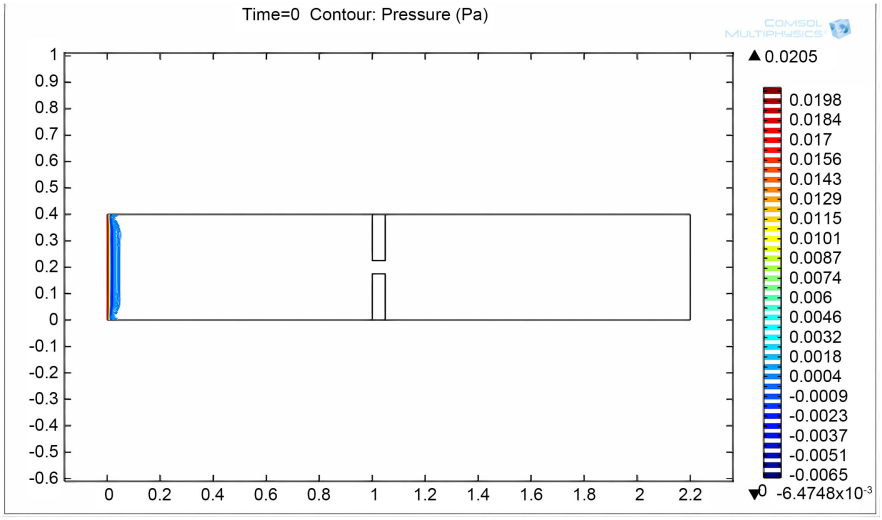

Figure 14. Contour pressure in the tank.

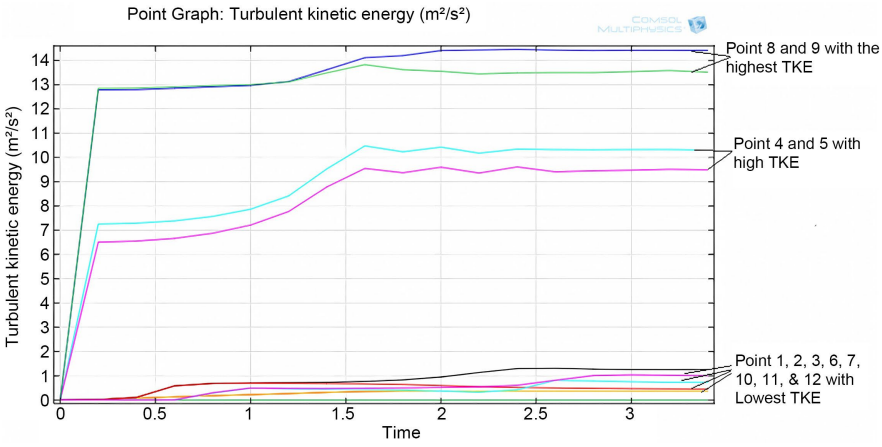

Figure 15. Turbulent kinetic energy point Graph for point 1 to 12 (see figure 5 above).

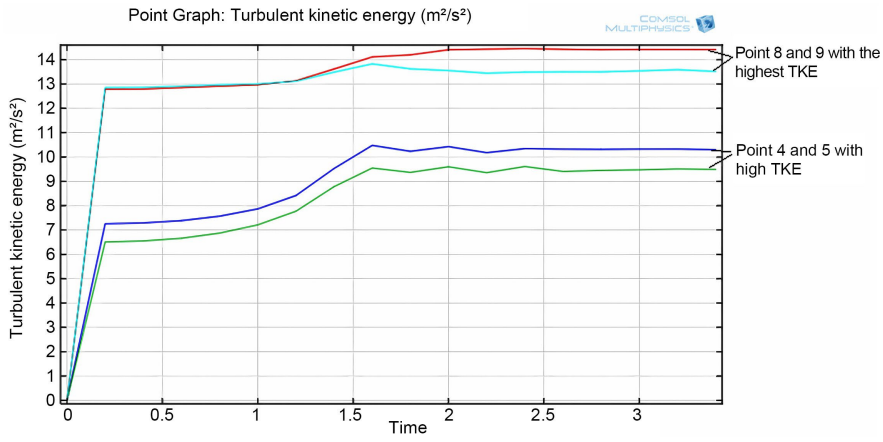

Figure 16. Turbulent kinetic energy point graph for point only for 4, 5, 8 and 9 (see figure 12 above).

6. Conclusion

The effects of fluid structure interactions (FSI) on baffles in tanks carried on

mobile trucks that, more often than not, experience sloshing phenomenon engulfed by turbulence behaviors with respect to different motions of the truck were studied. Mindful of the holes on baffles through which fluid passes, used in these tanks to limit sloshing wave activities, a single hole is evaluated and computed, showing the contour pressure and turbulent kinetic energy passing through a solver in COMSOL. The hole is discretized to point form such that the fluid flowing through each point is evaluated and interpreted on a point graph generated with respect to each point located on the tank or baffle hole. The result obtained shows a steady independent increase of turbulent kinetic energy (TKE) for points 4, 5, 8 and 9 for the first 0 to 0.25 seconds and then start fluctuating increasingly up to 3 seconds with the maximum TKE values reaching up to 14 m/s^2 and minimum values of 9.5 m/s^2. This, in real practical terms, means that there is more cohesion with the Fluid structure (baffle) interaction on the hole inlet area (point 4 and 5) and lesser at the outlet (point 8 and 9) on the Baffle. Generally, on these points more turbulent kinetic energy is at its maximum in the whole system. Also, TKE is felt on other points on the system with point further away having the least TKE this include point 1, 2, 3, 6, 7, 10, 11, and 12. Between 1.2 at 2.4 seconds, the highest TKE values were ranging from 0 to 1.4 m/s^2. This also means that there a lesser fluid particles velocity on these points. It is worth noting that improved results can be obtained in future while taking into consideration surface finishing, settlement surface inhibitors, and the Conicity of the baffle hole linked to concise geometrical tank data.

Conflicts of Interest

The authors declare no conflicts of interest regarding the publication of this paper.

References

[1] Cremonesi, M., Frangi, A. and Perego, U. (2010) A Lagrangian Finite Element Approach for the Analysis of Fluid-Structure Interaction Problems. *International Journal for Numerical Methods in Engineering*, **84**, 610-630. https://doi.org/10.1002/nme.2911

[2] Michler, C., Hulshoff, S.J., van Brummelen, E.H., de Borst, R. (2009) A Monolithic Approach to Fluid-Structure Interaction. *Computers & Fluids*, **33**, 839-848. https://doi.org/10.1016/j.compfluid.2003.06.006

[3] Ahamed, F., Atique, S., Munshi, A. and Koiranen, T. (2017) A Concise Description of One Way and Two Way Coupling Methods for Fluid-Structure Interaction Problems. *American Journal of Engineering Research*, **6**, 86-89. https://www.ajer.org/papers/v6(03)/O06038689.pdf

[4] Ayiehfor, C. (2024) The Effects of Fluid Sloshing on Different Baffle Configurations in Storage Tanks Transported on Trucks during an Emergency Braking. *Open Journal of Fluid Dynamics*, **14**, 24-63. https://doi.org/10.4236/ojfd.2024.141002

[5] Idelsohn, S.R. Oñate, E. and Del Pin, F. (2003) A Lagrangian Meshless Finite Element Method applied to Fluid-Structure Interaction Problems. *Computers and Structures*, **81**, 655-671. https://doi.org/10.1016/S0045-7949(02)00477-7

[6] Idelsohn, S.R., Oñate, E., Del Pin,F. and Calvo, N. (2006) Fluid-Structure Interaction

Using the Particle Finite Element Method. *Computer Methods in Applied Mechanics and Engineering*, **195**, 2100-2123. https://doi.org/10.1016/j.cma.2005.02.026

[7] Jog, C. S. and Pal, R. K. (2010) A Monolithic Strategy for Fuid-Structure Interaction Problems. *International Journal for Numerical Methods in Engineering*, **85**, 429-460. https://doi.org/10.1002/nme.2976

[8] Benra, F.-K., Dohmen, H.J., Pei, J., Schuster, S., and Wan, B. (2011) A Comparison of One-Way and Two-Way Coupling Methods for Numerical Analysis of Fluid-Structure Interactions. *Journal of Applied Mathematics*, 2011, Article ID: 853560. https://doi.org/10.1155/2011/853560

[9] Pedro, C. and Sibanda, P. (2012) An Algorithm for the Strong-Coupling of the Fluid-Structure Interaction Using a Staggered Approach. *Journal of Applied Mathematics*, **2012**, Article ID: 391974. https://doi.org/10.5402/2012/391974

[10] (2013) COMSOL Multiphysics 4.3b Model Library Manual. https://cn.comsol.com/sla

[11] Cadence, C.F.D. (2024) A Guide to Understanding Turbulent Kinetic Energy. https://resources.system-analysis.cadence.com/blog/msa2022-a-guide-to-understanding-turbulent-kinetic-energy

[12] Pope, S.B. (2000) Turbulent Flows. Cambridge University Press, 122-134. https://doi.org/10.1017/CBO9780511840531

[13] Baldocchi, D. (2005) Lecture 16, Wind and Turbulence, Part 1, Surface Boundary Layer: Theory and Principles. Ecosystem Science Division, Department of Environmental Science, Policy and Management, University of California.

[14] Boussinesq, J. (1877) Théorie de l'Ecoulement Tourbillant. *Mémoires presentés a L'Institut des Sciences*, **23**, 46-50.

[15] Davidson, L. (2022) An Introduction to Turbulence Models. https://www.tfd.chalmers.se/~lada/postscript_files/kompendium_turb.pdf

[16] Orrego, F., *et al.* (2012) Experimental and CFD Study of a Single Phase Cone-Shaped Helical Coiled Heat Exchanger: an Empirical Correlation. *Proceedings of ECOS* 2012 — *The* 25*th International Conference on Efficiency*, *Cost*, *Optimization*, *Simulation and Environmental Impact of Energy Systems*, Perugia, 26-29 June 2012, 3-9. https://www.academia.edu/2053469

[17] Wall, W.A. (2006) An Extended Finite Element Method Based Approach for Large Deformation Fluid-Structure Interaction. https://www.academia.edu/68478393/An_extended_finite_element_method_based_approach_for_large_deformation_fluid_structure_interaction?email_work_card=view-paper

[18] Elahi, R., Passandideh-Fard, M. and Javanshir, A. (2015) Simulation of Liquid Sloshing in 2D Containers Using the Volume of Fluid Method. *Ocean Engineering*, **96**, 226-244. https://doi.org/10.1016/j.oceaneng.2014.12.022

[19] Sayma, A. (2009) Computational Fluid Dynamics. https://kosalmath.wordpress.com/wp-content/uploads/2010/08/computational-fluid-dynamics.pdf